ARTICLE

Probing dynamics of carbon dioxide in a metal-organic framework under high pressure by high-resolution solid- state NMR

Munehiro Inukai,[*a] Takuya Kurihara,[b] Yasuto Noda,[b] Weiming Jiang,[b] Kiyonori Takegoshi,[b] Naoki Ogiwara,[b] Hiroshi Kitagawa,[b] and Koichi Nakamura[a]

The application of high-resolution NMR analysis for CO_2 adsorbed in an MOF under high pressure is reported for the first time. The results showed that CO_2 adsorbed in MOF-74 had a unusual slow mobility ($\tau \sim 10^{-8}$ s). CO_2–CO_2 interactions suppressed the mobility of CO_2 under high pressure, which, in turn, would have contributed to the stability of CO_2 at adsorption sites.

Introduction

Metal-organic frameworks (MOFs) and porous coordination polymers (PCPs) are an emerging class of nanoporous crystalline solids used to address the energy and environmental problems currently facing society.[1-3] Owing to their large surface area and adjustable pore sizes, MOFs have considerable uptake capacity and high selectivity. This makes them ideal for various applications, including as high pressure storage tanks for methane[4-7] and as membranes for CO_2 separation from pressurized H_2 and CO_2 matrices during pre-combustion CO_2 capture processes.[8, 9] Several studies on their uptake and selectivity under high pressure conditions have showed that host–guest (i.e., MOF–gas molecule) interactions strongly affected their uptake capacity and selectivity in low pressure environments, whereas guest–guest interactions contributed to their uptake under high pressure conditions dominantly.[10] Investigations into the various molecular interactions and their associated dynamics under high gas pressure have been key in understanding the adsorption process of MOFs;[11] however these studies have been less reported.

In this work, the dynamics of CO_2 in $[Zn_2(2,5\text{-DOTP})]_n$ (DOTP = 2,5-dioxidoterephthalate, MOF-74 or CPO-27) under high pressure was investigated using solid-state NMR. Solid-state NMR can be used to characterize locals structure of MOFs and dynamics of gas molecules in the pores.[12-14] MOF-74 is used as the representative MOF[15, 16] since it is known to have good selectivity toward CO_2 in pressurized gaseous mixtures.[17] CO_2 wobbling and hopping motions were analysed by ^{13}C solid-state NMR measurements using static NMR sample tubes containing

CO_2 and MOF-74.[11, 18, 19] In general, the NMR peaks of CO_2 and the frameworks of MOFs are broadened due to chemical shift anisotropy (CSA) and dipole–dipole interactions. This made it difficult to analyse the position and mobility of the adsorbed CO_2 as well as any local structural changes that might have taken place in the framework.

Herein, magic angle spinning NMR (MAS NMR) was performed under high pressure conditions. MAS NMR is a powerful solid-state NMR method that provides high-resolution spectra.[20, 21] In this particular case, an unusually slow mobility of CO_2 under high pressure conditions and a local structural changes which had occurred on the surface of MOF-74 were both revealed using this NMR technique.

Experimental

Materials

All chemicals employed were obtained from commercial suppliers and used without further purification. $[Zn_2(2,5\text{-DOTP})]_n$ was prepared as previously described.[15]

Measurements

X-ray powder diffraction (XRPD) patterns were collected on a Rigaku Miniflex 600 diffractometer with CuKα radiation. The adsorption and desorption isotherm of CO_2 at 298 K was collected by a high-pressure instrument (BELSORP-HP, MicrotracBEL Corp., Japan).

All solid state NMR measurements were performed in a magnet field of 7.16 T with a home-built spectrometer (OPENCORE spectrometer)[22] and a double resonance 5 mm magic angle spinning (MAS) probe. All ^{13}C NMR signals were acquired under Hahn-echo and two-pulse phase modulating (TPPM) proton decoupling. The recycle delays for ^{13}C NMR with or without CP were 4 s and 20 s. The contact time and spinning frequency were 8 ms and 6 kHz. Spin-lattice relaxation was measured by saturation recovery method.

[a.] Graduate School of Technology, Industrial and Social Sciences, Tokushima University, 2-1 Minami-Josanjima-Cho, Tokushima 770-8506, Japan.
E-mail: inukai.munehiro@tokushima-u.ac.jp

[b.] Division of Chemistry, Graduate School of Science, Kyoto University, Kitashirakawa-Oiwakecho, Sakyo-ku, Kyoto 606-8502, Japan.

† Footnotes relating to the title and/or authors should appear here.
Electronic Supplementary Information (ESI) available: [materials, XRD, adsorption isotherms, and solid-state NMR]. See DOI: 10.1039/x0xx00000x

Physical Chemistry Chemical Physics Accepted Manuscript

ARTICLE

Journal Name

MAS NMR for MOF samples under high pressure conditions

We fabricated a sample tube for high pressure MAS NMR measurements and a pressurized gas loading chamber as stated in previous studies (Fig. S1).[23-25] Activated MOF-74 was packed into the high pressure MAS NMR sample tube and the sample tube was put into the chamber in a glove bag. ^{13}C-enriched (99%) CO_2 was loaded into the chamber after evacuating the chamber. MOF-74 was exposed under CO_2 atmosphere for 2 h and sealed using a head cap screw with an O-ring (Fig. S1). When the sample tubes were prepared for other NMR experiments after the second time, the samples were heated at 433 K for 2 h to remove CO_2, exposed under CO_2 for 2h and sealed in the chamber. The maximum pressure and spinning frequency were 3.5 MPa and 6 kHz, respectively. The amount of CO_2 adsorbed in the MOF was estimated using high-pressure adsorption measurements (Fig. S3).

Simulations of ^{13}C CSA spectra

[13]C CSA spectra were simulated with EXPRESS[26] using combination of two types of jump model.[19, 27] The models were localized wobbling motion with the angle of α around primary site and hopping between primary sites with the angle of β with the rate of $k = 10^6$ Hz (Fig. S4).

T_1 analysis

T_1 analysis for adsorbed CO_2 were performed similar to our previous study.[28] The temperature-dependent τ_C were fitted to an Arrhenius equation, $\tau_C = \tau_0 \exp(E_a/RT)$, where τ_0, E_a, R, and T are pre-exponential factor, activation energy, the gas constant and temperature, respectively. We estimated τ_C and E_a from ^{13}C spin-lattice relaxation time (T_1) calculations. T_1 values were fitted by calculation curve based on Bloembergen-Purcell-Pound (BPP) theory.[29] We used CSA relaxation mechanism to calculate τ_C because the contribution from CSA to the T_1 of slow mobile CO_2 is much larger than that from the [1]H–[13]C dipole-dipole interaction. The CSA relaxation rate was $1/T_1(\text{CSA}) = (1/15)\gamma_C^2 B_0^2 (\Delta\sigma)^2 \left[2\tau_C/(1 + \omega_C^2\tau_C^2)\right]$, where γ_C, B_0, $\Delta\sigma$, and ω_C are gyromagnetic ratio, magnetic field, CSA and Larmor frequency, respectively. The CSA was $\Delta\sigma = -334.5$ ppm according to the literature.[30]

Results and discussion

Adsorption sites of MOF-74

MOF-74 has an analogous honeycomb structure which is composed of Zn^{2+} and DOTP. The structure contains 1D straight micropores that are approximately 11 Å in diameter with unsaturated metal sites (open metal site: OMS) at the corner of the pores that are available for coordination. The OMS functions as a Lewis acid site which results in excellent adsorption and separation behavior in CO_2. Adsorption sites located at the OMS (primary site), the DOTP (secondary site) and the center of the pores (tertiary sites) have been identified by room temperature neutron diffraction experiments (Fig. 1).[31-33] Whereas the primary sites strongly bonded CO_2 with the

help of coordination bonds, CO_2 adsorbed at the secondary sites were stabilized via intermolecular interactions of the CO_2 molecules adsorbed at the primary site. Once full occupancy was achieved at the primary and secondary sites, CO_2 adsorption then occurred at the tertiary sites.
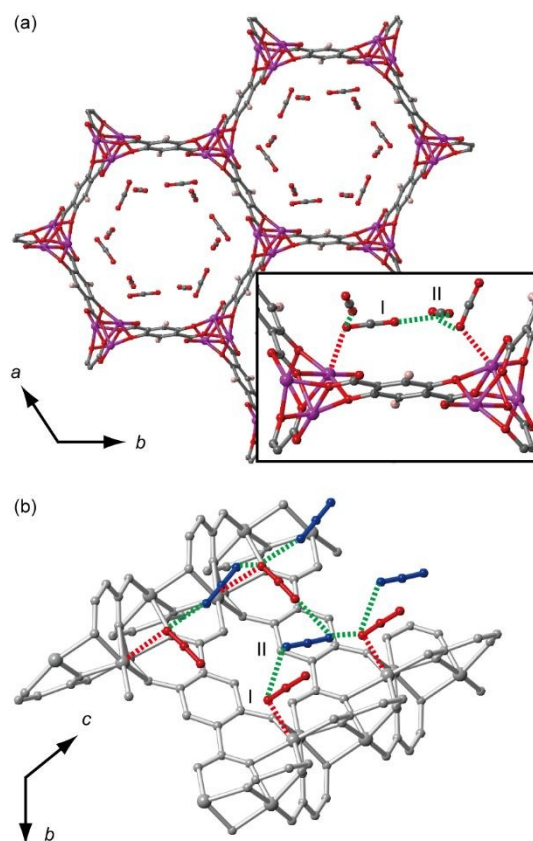

Fig. 1 (a) Adsorption sites on MOF-74. Purple, red, black and light pink colors represent Zn, O, C and H, respectively. (b) Cross-section of the 1D channel of MOF-74. Red and blue represent adsorbed CO_2 at the primary and secondary sites, respectively. The hydrogen atoms and the tertiary sites have been omitted for clarity. The coordination bonds as well as the interactions between CO_2 and its nearest neighbors are drawn as red and green dotted lines, respectively.

^{13}C CSA NMR analyses

^{13}C CSA NMR measurements for static-state NMR sample were carried out to probe the dynamics of the adsorbed CO_2. CSA is useful for studying the hopping and the rotational mode in molecules. Previous CSA studies have reported that the two types of CO_2 dynamics exist at low CO_2 pressures: "localized wobbling" at an angle of α around the primary site and "hopping" occurred between the primary sites at an angle of β (Fig. S4).[19] The α–angle was defined as the angle between the long axis of CO_2 and the wobbling axis, whereas the β–angle was the angle between the long axis of CO_2 and the c-axis of MOF-74. CSA patterns of CO_2 adsorbed in MOF-74 at pressures ranging between 0.01 and 1.0 MPa are shown in Fig. 2a. Simulation of CSA patterns were carried out with fast motion limits (i.e., $k \geq 10^6$ Hz) for assuming the local wobbling and hopping motions (see supplementary information). The patterns observed at 0.01 and 0.05 MPa were almost identical to the simulated patterns, and the angles seen in our study were

ARTICLE

similar to those in previous NMR analyses (e.g. $\alpha = 30°$ and $\beta = 60°$ at 0.3 CO_2/Zn^{2+}).[27] Other complicated dynamics, such as the distribution of the angles and the presence of other hopping sites (i.e., primary–second and second–second sites) would exist at pressure conditions above 0.1 MPa. It was difficult to perform NMR analyses that accurately reflect these additional motions. An additional peak, which was attributed to the gaseous phase of CO_2, also appeared at around 124.5 ppm in the spectrum acquired at 1.0 MPa. With every incremental change in pressure, the top of the peak in the spectrum shifted from the right to the left, a trend that is similarly observed in previous NMR and DFT studies conducted on Mg-MOF-74 heavily loaded with CO_2.[11] This change indicates that there is a corresponding decrease in the averaged β–angle because the β-angle dictates the line shape (Fig. S5). Intermolecular interactions between CO_2 trigger orientation of the CO_2 molecules toward the c-axis under high pressure conditions.
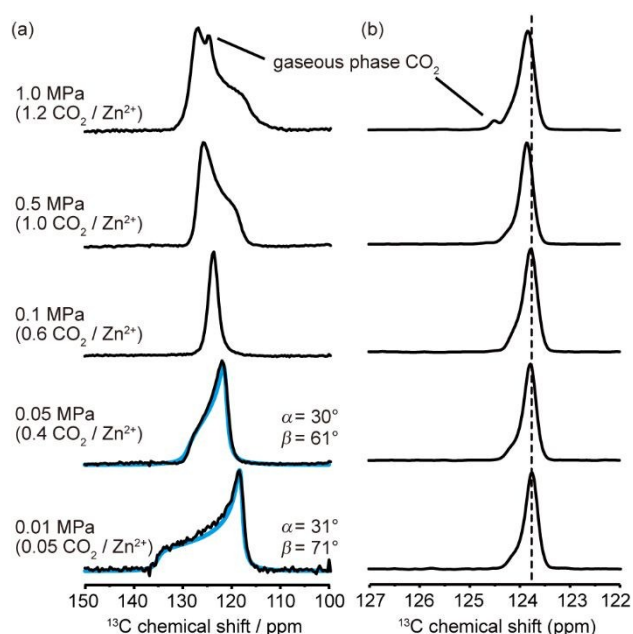
**Fig. 2** (a) ^{13}C CSA NMR and (b) MAS NMR spectra for CO_2 adsorbed in MOF-74 at 305 K and at pressures ranging from 0.01 to 1.0 MPa. Black and blue lines correspond to the experimental and simulated spectra, respectively. Simulated spectra reflect localized wobbling at the α angle around the primary sites and 6-site hopping between the primary sites at the β angle.

^{13}C MAS NMR analyses

In addition to the results of the CSA analyses, high-resolution MAS NMR spectra provided information on the position and the dynamics of the CO_2 molecules. A large peak at 123.8 ppm with a small shoulder at around 124.1 ppm appeared in the spectrum acquired at 0.01 MPa; it was assigned to CO_2 molecules that were adsorbed at the primary site since there were very few absorbed CO_2 in the pores. The shoulder of the peak exhibited broadening typically attributed to inhomogeneity in the magnetic field caused by the fabricated sample tube (Fig. S7a). An additional peak at 124.5 ppm appeared in the spectrum acquired at 1.0 MPa was due to gaseous phase (free mobile) CO_2 molecules. A gradual downfield shift was observed with increasing pressure. All spectra obtained at pressures ranging

from 0.05 to 1.0 MPa showed only one peak for adsorbed CO_2 despite the presence of different types of CO_2 attributing to the adsorption on primary sites and secondary sites. CO_2 adsorbed on secondary sites would have slightly higher chemical shift than 123.8 ppm. These two types of CO_2 would exchange within the NMR time scale (at an order of tens of milliseconds), leading to a single peak at around 123.8 ppm. Shifts in the peak's position implies that there are incremental changes in the population of CO_2 adsorbed at the secondary sites.
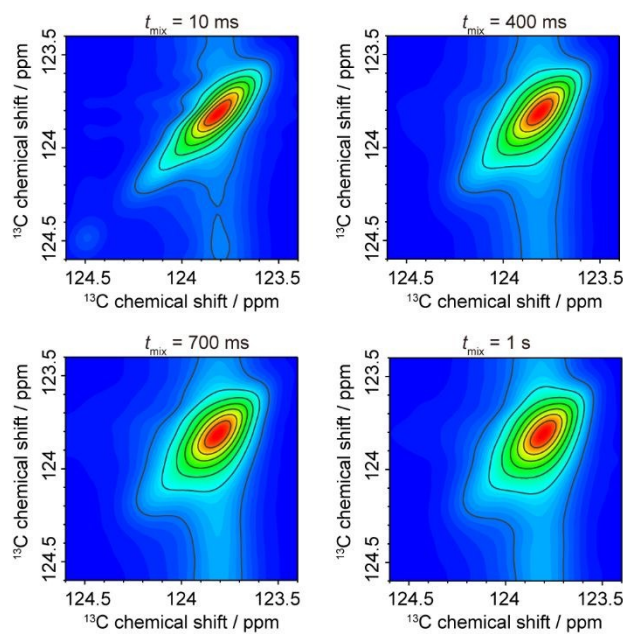
Fig. 3 ^{13}C 2D exchange MAS NMR spectra for CO_2 in MOF-74 under 1.0 MPa. The mixing times were 10, 400, 700 ms and 1s, respectively.

^{13}C 2D exchange MAS NMR measurements for CO_2 adsorbed in MOF-74 at 1.0 MPa were conducted with a mixing time of 10-1000 ms to investigate diffusion of CO_2. The spectra showed that there was no exchange between the peaks at 123.8 and 124.5 ppm (Fig. 3). This suggests that the peak observed at 124.5 ppm is not attributed to the CO_2 molecules adsorbed at the tertiary sites, but rather to the gaseous phase CO_2 located in the dead space of the NMR sample tube. Moreover, the shape of 2D spectra gradually rounded with every increase in the mixing time. This means that the location of CO_2 seen at 123.8 ppm and 124.1 ppm are in exchange. The observed spectral change is indicative of CO_2 diffusion throughout the NMR sample tube within several hundred milliseconds because the shoulder peak reflects the distribution of adsorbed CO_2 in the NMR sample tube.

T_1 analyses

Longitudinal relaxation time (T_1) analyses were performed for the peak observed at 123.8 ppm to quantitatively evaluate the mobility of CO_2. The T_1 values gradually increased with rising pressure (Fig. 4a). This pressure dependence indicates that the mobility of CO_2 under high pressure is restricted by extensive CO_2–CO_2 interactions. This restriction in mobility would have contributed to the stability of the adsorption process. To

determine the activation energy and correlation time corresponding to one rotation period of CO_2, we also carried out T_1 analyses from 305 to 363 K with 0.1 and 1.0 MPa (Fig. 4b); in both cases, the T_1 values decreased with an increase in temperature. The correlation times calculated at 305 K, pre-exponential factors and activation energies were $1.8(5) \times 10^{-8}$ s, $3.2(5) \times 10^{-9}$ s and 4.4(4) kJ/mol (at 0.1 MPa), and $3.2(4) \times 10^{-8}$ s, $8(1) \times 10^{-9}$ s and 3.5(4) kJ/mol (at 1.0 MPa), respectively. In the T_1 measurement at 1.0 MPa, the activation energy was relatively lower and the pre-exponential factor was higher than those at 0.1 MPa. The result would indicate that the population of CO_2 adsorbed on secondary sites and the frequency of collision between molecules (CO_2– CO_2 and CO_2–pores surface) increase with an increase in pressure. The correlation time was much longer than that of gaseous phase CO_2 and comparable to the values of solid state materials such as polymer chains.[34, 35] Notably, the correlation time at 0.1 MPa was 100-fold larger than that of Mg-MOF-74 (1.1×10^{-10} s at 0.5 CO_2/Mg^{2+} calculated using the Arrhenius equation) based on T_1 analyses.[18] As an extension of this study, we have a prospect to perform MAS NMR for other M^{2+}–MOF-74 (where M = Mg, Mn, Co, Ni, Cu and Fe) under various CO_2 pressure parameters in order to have a systematic study in mobility, adsorption and separation properties. Thus far, CSA and T_1 analyses have proven that the adsorbed CO_2 molecules underwent localized wobbling at the adsorption sites and hopping between the adsorption sites at a rate of 10^{-8} s. 2D exchange MAS NMR analyses have revealed the diffusion of CO_2 among the particles in the NMR sample tube at a rate of 10^{-1} s.
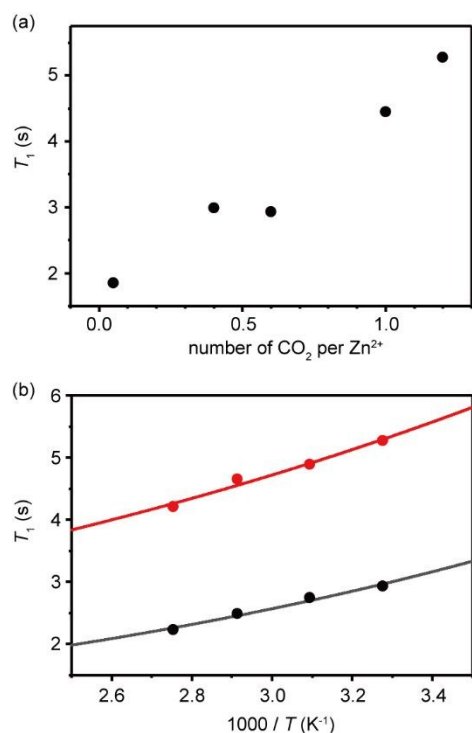

Fig. 4 (a) Pressure and (b) temperature dependence of T_1 values for the adsorbed CO_2 at 305 K and at 0.1 MPa (black) and 1.0 MPa (red), respectively. Circles and solid lines represent the experimental and calculated T_1 values, respectively.

^{13}C CP-MAS NMR analyses

To monitor the local structure of the framework under high pressure conditions, ^1H–^{13}C cross-polarization MAS (CP-MAS) NMR of MOF-74 was carried out from 0.01 to 1.0 MPa (Fig. 5). In the resulting spectra, C1 (seen at 123 ppm), C2 (126 ppm), C3 (156 ppm) and C4 (156 ppm) were assigned to the phenyl ring, the hydroxo and the carboxylate functional groups of DOTP, whereas the peaks of adsorbed CO_2 molecules did not appear at all; this is because CP-MAS spectra only reflected the rigid molecules in solid materials. No obvious peak's shifts were observed with increasing pressure, suggesting that the framework remained intact under high pressure. The spectra showed a broad peak between 160 and 170 ppm (B1) which did not appear in the spectra acquired for natural isotopic abundance CO_2 adsorbed in MOF-74 (Fig. S7b). This peak would be attributed to the carbon of carbamate originating from chemisorbed CO_2. The dimethylamine derived from the decomposition of DMF during the synthesis may be trapped in the pores and formed the carbamate with CO_2 during adsorption.[36, 37]
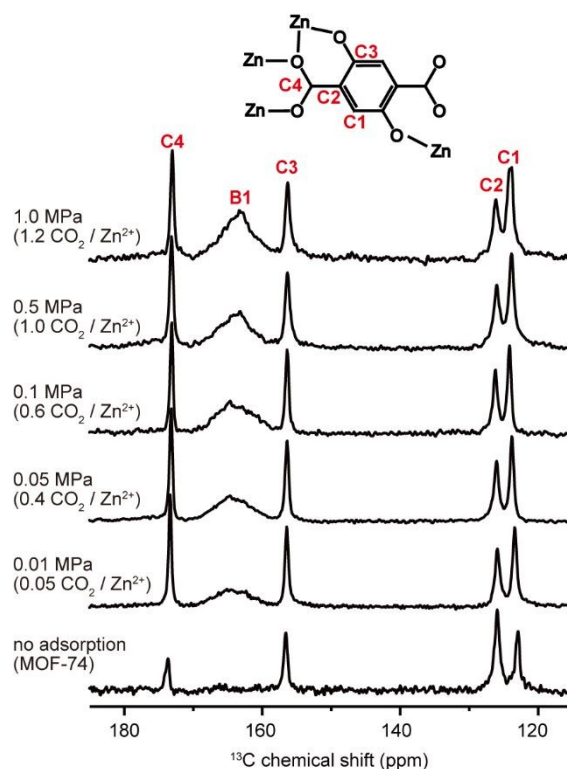
Fig. 5 ^{13}C CP-MAS NMR spectra of MOF-74 CO_2 at 305 K at pressures ranging from 0.01 to 1.0 MPa.

Conclusions

In summary, the dynamics of CO_2 adsorbed in MOF-74 under high pressure was investigated using CSA and MAS NMR analyses. T_1 analyses revealed that the occurrence of unusually slow localized wobbling and hopping motions at a rate of 10^{-8} s. Mobility of the CO_2 molecules decreased with every incremental rise in pressure due to the presence of extensive

Journal Name

ARTICLE

CO_2–CO_2 interactions. Suppression of this motion would increase the stability of CO_2 molecules at the adsorption sites. Moreover, the high resolution MAS NMR spectra revealed the diffusion of CO_2 among the particles at a rate of 10^{-1} s and the existence of carbamate originating from CO_2 in the pores. These results contribute to understanding of the adsorption and separation processes for MOFs subjected to high pressure conditions.

Conflicts of interest

There are no conflicts to declare.

Acknowledgements

Notes and references

1   O. M. Yaghi, M. O'Keeffe, N. W. Ockwig, H. K. Chae, M. Eddaoudi and J. Kim, *Nature*, 2003, **423**, 705-714.
2   S. Kitagawa, R. Kitaura and S.-i. Noro, *Angew. Chem. Int. Ed.*, 2004, **43**, 2334-2375.
3   G. Férey, C. Mellot-Draznieks, C. Serre and F. Millange, *Acc. Chem. Res.*, 2005, **38**, 217-225.
4   J. A. Mason, J. Oktawiec, M. K. Taylor, M. R. Hudson, J. Rodriguez, J. E. Bachman, M. I. Gonzalez, A. Cervellino, A. Guagliardi, C. M. Brown, P. L. Llewellyn, N. Masciocchi and J. R. Long, *Nature*, 2015, **527**, 357.
5   F. Moreau, D. I. Kolokolov, A. G. Stepanov, T. L. Easun, A. Dailly, W. Lewis, A. J. Blake, H. Nowell, M. J. Lennox, E. Besley, S. Yang and M. Schröder, *Proc. Natl. Acad. Sci. USA.*, 2017, **114**, 3056-3061.
6   S. Bracco, D. Piga, I. Bassanetti, J. Perego, A. Comotti and P. Sozzani, *J. Mater. Chem. A*, 2017, **5**, 10328-10337.
7   K. Shao, J. Pei, J.-X. Wang, Y. Yang, Y. Cui, W. Zhou, T. Yildirim, B. Li, B. Chen and G. Qian, *Chem. Commun.*, 2019, **55**, 11402-11405.
8   A. R. Millward and O. M. Yaghi, *J. Am. Chem. Soc.*, 2005, **127**, 17998-17999.
9   Z. R. Herm, J. A. Swisher, B. Smit, R. Krishna and J. R. Long, *J. Am. Chem. Soc.*, 2011, **133**, 5664-5667.
10 J. Y. Jung, F. Karadas, S. Zulfiqar, E. Deniz, S. Aparicio, M. Atilhan, C. T. Yavuz and S. M. Han, *Phys. Chem. Chem. Phys.*, 2013, **15**, 14319-14327.
11 R. M. Marti, J. D. Howe, C. R. Morelock, M. S. Conradi, K. S. Walton, D. S. Sholl and S. E. Hayes, *J. Phys. Chem. C*, 2017, **121**, 25778-25787.
12 B. E. G. Lucier, S. Chen and Y. Huang, *Acc. Chem. Res.*, 2018, **51**, 319-330.
13 Y. T. A. Wong, V. Martins, B. E. G. Lucier and Y. Huang, *Eur. J. Chem.*, 2019, **25**, 1848-1853.
14 V. J. Witherspoon, J. Xu and J. A. Reimer, *Chem. Rev.*, 2018, **118**, 10033-10048.
15 N. L. Rosi, J. Kim, M. Eddaoudi, B. L. Chen, M. O'Keeffe and O. M. Yaghi, *J. Am. Chem. Soc.*, 2005, **127**, 1504-1518.
16 P. D. C. Dietzel, R. E. Johnsen, R. Blom and H. Fjellvag, *Chem. Eur. J.*, 2008, **14**, 2389-2397.

17 J. A. Mason, K. Sumida, Z. R. Herm, R. Krishna and J. R. Long, *Energy Environ. Sci.*, 2011, **4**, 3030-3040.
18 X. Kong, E. Scott, W. Ding, J. A. Mason, J. R. Long and J. A. Reimer, *J. Am. Chem. Soc.*, 2012, **134**, 14341-14344.
19 L. C. Lin, J. Kim, X. Kong, E. Scott, T. M. McDonald, J. R. Long, J. A. Reimer and B. Smit, *Angew. Chem. Int. Ed.*, 2013, **52**, 4410-4413.
20 M. Mehring, *High resolution NMR spectroscopy in solids*, Springer, New York, 1976.
21 C. P. Slichter, *Principles of Magnetic Resonance 3rd edn*, Springer, New York, 1990.
22 K. Takeda, *J. Magn. Reson.*, 2008, **192**, 218-229.
23 D. W. Hoyt, R. V. Turcu, J. A. Sears, K. M. Rosso, S. D. Burton, A. R. Felmy and J. Z. Hu, *J. Magn. Reson.*, 2011, **212**, 378-385.
24 R. V. Turcu, D. W. Hoyt, K. M. Rosso, J. A. Sears, J. S. Loring, A. R. Felmy and J. Z. Hu, *J. Magn. Reson.*, 2013, **226**, 64-69.
25 J. Z. Hu, M. Y. Hu, Z. Zhao, S. Xu, A. Vjunov, H. Shi, D. M. Camaioni, C. H. F. Peden and J. A. Lercher, *Chem. Commun.*, 2015, **51**, 13458-13461.
26 R. L. Vold and G. L. Hoatson, *J. Magn. Reson.*, 2009, **198**, 57-72.
27 W. D. Wang, B. E. Lucier, V. V. Terskikh, W. Wang and Y. Huang, *J. Phys. Chem. Lett.*, 2014, **5**, 3360-3365.
28 M. Inukai, M. Tamura, S. Horike, M. Higuchi, S. Kitagawa and K. Nakamura, *Angew. Chem. Int. Ed.*, 2018, **57**, 8687-8690.
29 N. Bloembergen, E. M. Purcell and R. V. Pound, *Phys. Rev.*, 1948, **73**, 679-712.
30 A. J. Beeler, A. M. Orendt, D. M. Grant, P. W. Cutts, J. Michl, K. W. Zilm, J. W. Downing, J. C. Facelli, M. S. Schindler and W. Kutzelnigg, *J. Am. Chem. Soc.*, 1984, **106**, 7672-7676.
31 H. Wu, J. M. Simmons, G. Srinivas, W. Zhou and T. Yildirim, *J. Phys. Chem. Lett.*, 2010, **1**, 1946-1951.
32 W. L. Queen, C. M. Brown, D. K. Britt, P. Zajdel, M. R. Hudson and O. M. Yaghi, *J. Phys. Chem. C*, 2011, **115**, 24915-24919.
33 W. L. Queen, M. R. Hudson, E. D. Bloch, J. A. Mason, M. I. Gonzalez, J. S. Lee, D. Gygi, J. D. Howe, K. Lee, T. A. Darwish, M. James, V. K. Peterson, S. J. Teat, B. Smit, J. B. Neaton, J. R. Long and C. M. Brown, *Chem. Sci.*, 2014, **5**, 4569-4581.
34 M. H. Levitt, *Spin dynamics: basics of nuclear magnetic resonance*, Wiley, Chichester, England, 2001.
35 V. I. Bakhmutov, *Practical NMR Relaxation for Chemists*, Wiley, Chichester, England, 2005.
36 A. C. Forse, P. J. Milner, J. H. Lee, H. N. Redfearn, J. Oktawiec, R. L. Siegelman, J. D. Martell, B. Dinakar, L. B. Porter-Zasada, M. I. Gonzalez, J. B. Neaton, J. R. Long and J. A. Reimer, *J. Am. Chem. Soc.*, 2018, **140**, 18016-18031.
37 R. L. Siegelman, P. J. Milner, A. C. Forse, J. H. Lee, K. A. Colwell, J. B. Neaton, J. A. Reimer, S. C. Weston and J. R. Long, *J. Am. Chem. Soc.*, 2019, **141**, 13171-13186.